Amino Acid Sequence and Carbohydrate Structure of a Recombinant Human Tissue Factor Pathway Inhibitor Expressed in Chinese Hamster Ovary Cells: One *N*- and Two *O*-Linked Carbohydrate Chains Are Located between Kunitz Domains 2 and 3 and One *N*-Linked Carbohydrate Chain Is in Kunitz Domain 2[†]

Yo Nakahara,[‡] Toshiyuki Miyata,[§] Tsutomu Hamuro,[‡] Akinobu Funatsu,[‡] Masaru Miyagi,[∥] Susumu Tsunasawa,[∥] and Hisao Kato*,[§]

The Chemo-Sero-Therapeutic Research Institute, Shimizumachi, Ohkubo 668, Kumamoto 860; National Cardiovascular Center Research Institute, Fujishirodai 5, Suita, Osaka 565, and Laboratories of Biotechnology Research, Takara Shuzo Co., Ltd., Seta 3-4-1, Otsu, Shiga 520-21, Japan

Received October 18, 1995; Revised Manuscript Received March 15, 1996[⊗]

ABSTRACT: Human tissue factor pathway inhibitor is a protease inhibitor with three tandem Kunitz-type inhibitory domains. The recombinant protein (r-hTFPI) was produced using Chinese hamster ovary cells, and its polypeptide and carbohydrate chain structures were analyzed. The complete amino acid sequence, composed of 276 residues, was determined using a protein sequencer after protease digestion and it was identical to that predicted from the cDNA sequence. Among three potential *N*-glycosylation sites, both Asn^{117} and Asn^{167} were fully *N*-glycosylated but Asn^{228} was not. Thr^{175} was also fully *O*-glycosylated, but Ser^{174} was partially *O*-glycosylated. Carbohydrate composition and mass spectrometric analyses of the undecapeptide OG-11 (residues Leu^{170}∼Leu^{180}) showed that two *O*-linked carbohydrate chains consisted of a type-1 core structure (Gal-GalNAc-Ser/Thr) with 0−3 mol of *N*-acetylneuraminic acid(s). The *N*-linked carbohydrate chains were analyzed by two-dimensional carbohydrate mapping combined with sequential glycosidase digestion, after the reducing-ends of carbohydrate residues were tagged with 2-aminopyridine and non-reducing-end sialic acids were removed with sialidase. All the *N*-linked structures in r-hTFPI were complex-type carbohydrate chains with one fucose residue attached to the reducing-end GlcNAc and consisted of bi-, tri-, and tetraantennary carbohydrate chains in the ratio 1.9:1.3:1.0. Fucosylated tri- and tetraantennary carbohydrate chains with one or two *N*-acetyllactosaminyl repeats were also found (30% of carbohydrate chains determined). Thus, the region between Kunitz domains 2 and 3 encoded by exon 7 was highly glycosylated by two *O*-linked carbohydrate chains at Ser^{174} and Thr^{175} and one *N*-linked carbohydrate chain at Asn^{167}. These results indicated that the region is occupied by a cluster of three bulky and acidic carbohydrate chains.

Tissue factor pathway inhibitor (TFPI)[1] is a Kunitz-type protease inhibitor with three tandem inhibitory domains (Kunitz domains 1−3). TFPI inhibits the initial reactions of the tissue factor-mediated blood coagulation pathway, interacting with factor Xa via Kunitz domain 2 and with the tissue factor−factor VIIa complex via Kunitz domain 1 [see review by Broze et al. (1990)]. TFPI uniquely binds lipoproteins, heparin, and proteoglycans on vascular endothelial cells, which are supposed to be mediated at least by Kunitz domain 3 and the carboxy-terminal basic domain of TFPI (Valentin et al., 1993; Enjyoji et al., 1995). Human recombinant TFPI has been expressed in various cells, including *Escherichia coli* (Diaz-Collier et al., 1994), yeast (Petersen et al., 1993), and mammalian cells from CHO (Wun et al., 1992; Enjyoji et al., 1995), mouse C127, baby hamster kidney, and SK hepatoma (Wun et al., 1992). The structure and function of TFPI has been studied using recombinant full-length and truncated TFPI [see reviews by Lindahl et al. (1992), Novotny (1994), Petersen et al. (1995), Broze (1995), and Wun (1995)]. The potential use of recombinant TFPI as a new anticoagulant reagent has been proven in experimental, reconstituted systems and also in animal models.

Although TFPI has three potential *N*-glycosylation sites, their structures have not been studied on both recombinant and plasma-derived TFPI. The carbohydrate portions of glycoproteins play important roles in their stability, susceptibility toward proteases, turnover rate, and probably in interactions with proteins and carbohydrates, such as lipoproteins, heparin, and proteoglycan. Since it is very difficult to obtain a large quantity of plasma-derived TFPI, we investigated the structures of carbohydrate and glycosylation sites of recombinant TFPI from CHO cells and tried to extend

[†] This work was supported in part by Special Coordination Funds for Promoting Science and Technology (Encouragement System of COE), the Science and Technology Agency of Japan.

* To whom correspondence should be addressed. Tel: +81-6-833-5012, ext 2512. FAX: +81-6-872-7485.

[‡] The Chemo-Sero-Therapeutic Research Institute.

[§] National Cardiovascular Center Research Institute.

[∥] Takara Shuzo Co., Ltd.

[⊗] Abstract published in *Advance ACS Abstracts,* May 1, 1996.

[1] Abbreviations: CHO, Chinese hamster ovary; Fuc, fucose; GalNAc, *N*-acetylgalactosamine; GlcNAc, *N*-acetylglucosamine; Gal, galactose; Hex, hexose; HexNAc, *N*-acetylhexosamine; HPLC, high-performance liquid chromatography; LacNAc, *N*-acetyllactosamine; Man, mannose; NeuAc, *N*-acetylneuraminic acid; PA, pyridylamino; PTC, phenylthiocarbamoyl; PTH, phenylthiohydantoin; r-hTFPI, recombinant human tissue factor pathway inhibitor; RP-HPLC, reversed phase high-performance liquid chromatography; Sia, sialic acid; Da, dalton.

S0006-2960(95)02488-3 CCC: $12.00 © 1996 American Chemical Society

this information to plasma-derived TFPI. In this study, we found that one of three potential *N*-glycosylation sites is not glycosylated and we identified two additional *O*-glycosylation sites. We determined their carbohydrate structures by HPLC and mass spectrometry and revealed that a cluster of carbohydrate chains is present between Kunitz domains 2 and 3 of TFPI.

EXPERIMENTAL PROCEDURES

Materials. Human r-TFPI was expressed in CHO cells and purified as described (Enjyoji et al., 1995). Lysylendopeptidase (*Achromobacter* protease I) and thermolysin were purchased from Wako Pure Chemical Industries (Osaka, Japan). V8 (*Staphylococcus aureus*) protease was from ICN Biomedicals (Costa Mesa, CA). Bovine kidney α-L-fucosidase was purchased from Boehringer Mannheim (Tokyo, Japan). Sialidase (*Arthrobacter ureafaciens*) was from Nacalai Tesque Inc. (Kyoto, Japan). β-Galactosidase and β-*N*-acetylhexosaminidase from jack bean and endo-β-galactosidase from *Escherichia freundii* were purchased from Seikagaku Kogyo Co., Ltd. (Tokyo, Japan). PA−sugar chains were purchased from Takara Shuzo Co., Ltd. (Shiga, Japan) or Nakano Vinegar Co., Ltd. (Aichi, Japan). All other chemicals were analytical grade or of the highest quality commercially available.

Preparation of Peptides for Sequence Analysis. A sample containing 1.1 mg (23 nmol) of r-hTFPI was reduced with dithiothreitol and then *S*-pyridylethylated by the addition of 4-vinylpyridine. After dialysis against water, half of the sample was digested with lysylendopeptidase at a 1:100 weight ratio overnight at 37 °C in 50 mM Tris-HCl buffer, pH 9.0, containing 4 M urea and the other half was digested with V8 protease at a 1:25 weight ratio overnight at 37 °C in 0.1 M NH_4HCO_3 containing 2 M urea. They were separated on a column of COSMOSIL 5C18-300 (4.6 × 150 mm, Nacalai Tesque, Inc., Kyoto, Japan) at a flow rate of 0.5 mL/min, using a Waters model 625 LC system equipped with a Waters 991J photodiode array detector. Peptides were eluted with a linear gradient of 0%−40% acetonitrile in 0.05% trifluoroacetic acid for 40 min and 40%−80% acetonitrile in 0.05% trifluoroacetic acid for the next 10 min. The peak fractions were collected manually, and peptides were analyzed by amino acid analysis. Fractions containing two or more peptides were further purified using a Waters μBondasphere C18 (5 μm, 300 Å, 2.1 × 150 mm) and/or C8 (5 μm, 300 Å, 2.1 × 150 mm) column under the same conditions described above except for the flow rate, which was 0.2 mL/min.

Amino Acid Composition and Sequence Analysis. Samples were hydrolyzed in 5.7 M hydrochloric acid containing 1% phenol in evacuated sealed tubes at 110 °C for 20 h, converted to PTC derivatives, and then PTC-amino acids were quantified using a Waters Pico-Tag system (Heinrikson & Meredith, 1984). The amino acid sequence of each peptide was determined using an Applied Biosystems model 473A protein sequencer (Foster City, CA), equipped with a model 610A data analysis system.

Sugar Composition Analysis. A dried sample (0.01−10 nmol of sugars or a glycopeptide) was hydrolyzed using a mixture of equal amounts of 4 M trifluoroacetic acid and 4 M hydrochloric acid under reduced pressure at 100 °C for 4 h in a sealed tube. After acetylation of the free amino groups, the hydrolysate was pyridylaminated using a PALSTATION model 1000 (Takara Shuzo Co.) with CA5100 pyridylamination reagent kits (Takara Shuzo Co.). The reaction mixture was dissolved in water, and a portion of the solution was analyzed by anion-exchange HPLC with a PALPAK Type-A (4.6 mm × 150 mm, Takara Shuzo Co., Ltd.) column (Takemoto et al., 1985; Suzuki et al., 1991).

Preparation of O-Glycosylated Peptide. Reduced and *S*-pyridylethylated r-hTFPI (about 20 nmol) was digested with lysylendopeptidase, and the digests were separated by RP-HPLC as described above. The fraction containing peptide K12−13, in which main contaminant was peptide K8−9, was evaporated and dissolved in 100 μL of 0.2 M $HCOONH_4$ buffer (pH 7.0) containing 8 M urea. Thereafter, 68 μL of distilled water and 32 μL of 1 mg of thermolysin/mL in 50% glycerol were added. After a 16 h incubation at 37 °C, the digest was separated using RP-HPLC (COSMOSIL 5C18-300) with a linear gradient of acetonitrile from 0% to 40% within 80 min. To identify the peptide carrying *O*-linked sugar chains, aliquots of each peak were dried and acid hydrolyzed. The hydrolysate was derivatized with phenylisothiocyanate, and the GalNAc content was analyzed using a Pico-Tag amino acid analyzer.

Mass Spectrometric Analysis. Mass spectrometric analysis was performed using a PE-Sciex API-III triple-quadrupole mass spectrometer (Ontario, Canada) equipped with an ionspray ion source in the positive mode. The molecular mass of peptide OG-11 dissolved in 100 μL of 0.05% TFA-acetonitrile (1:1) was measured by introducing the glycopeptide into the mass spectrometer through a fused silica tube (100 μm i.d.) at a flow rate of 2 μL/min. The daughter ion spectrum of OG-11 was obtained in the triple-quadrupole daughter scan mode by selectively introducing OG-11 (*m*/*z* 1388.4) from Q1 into the collision cell (Q2) and observing the daughter ions in Q3. The resolution of Q1 and Q3 was about 500 and 1500, respectively.

Preparation of N-Linked Carbohydrate Chains. N-Linked carbohydrate chains were liberated by the hydrazinolysis (100 °C, 10 h) of about 2.4 mg of r-hTFPI, and their free amino groups were *N*-acetylated as reported (Hase et al., 1984). The reducing ends of the carbohydrate chains were pyridylaminated without the loss of sialic acid residues (Kondo et al., 1990) using a PALSTATION model 1000 with CA5000 pyridylamination reagent kits (Takara Shuzo Co., Ltd.). The pyridylamino derivatives of carbohydrate chains thus obtained were purified by gel filtration on a Sephadex G-15 column (8 × 200 mm: Pharmacia Biotech, Tokyo, Japan) equilibrated with 10 mM acetic acid and then digested with 1 unit of sialidase from *Arthrobactor ureafaciens* in 0.5 mL of 0.1 M acetate buffer (pH 5.0). To confirm the removal of sialic acid from the carbohydrate chains, a portion was separated by HPLC using an anion-exchange column containing PALPAK Type-N (Takara Shuzo Co., Ltd.). Carbohydrate chains were eluted by a linear gradient from 0% to 55% solvent B for 110 min at a flow rate of 1.0 mL/min at 40 °C, using a two-solvent-system: 50 mM triethylamine-acetic acid (pH 7.3) containing 40% acetonitrile as solvent A and 1 M triethylamine-acetic acid (pH 7.3) containing 50% acetonitrile as solvent B. Carbohydrate chains were identified using a fluorescence detector with excitation at 310 nm and emission at 380 nm.

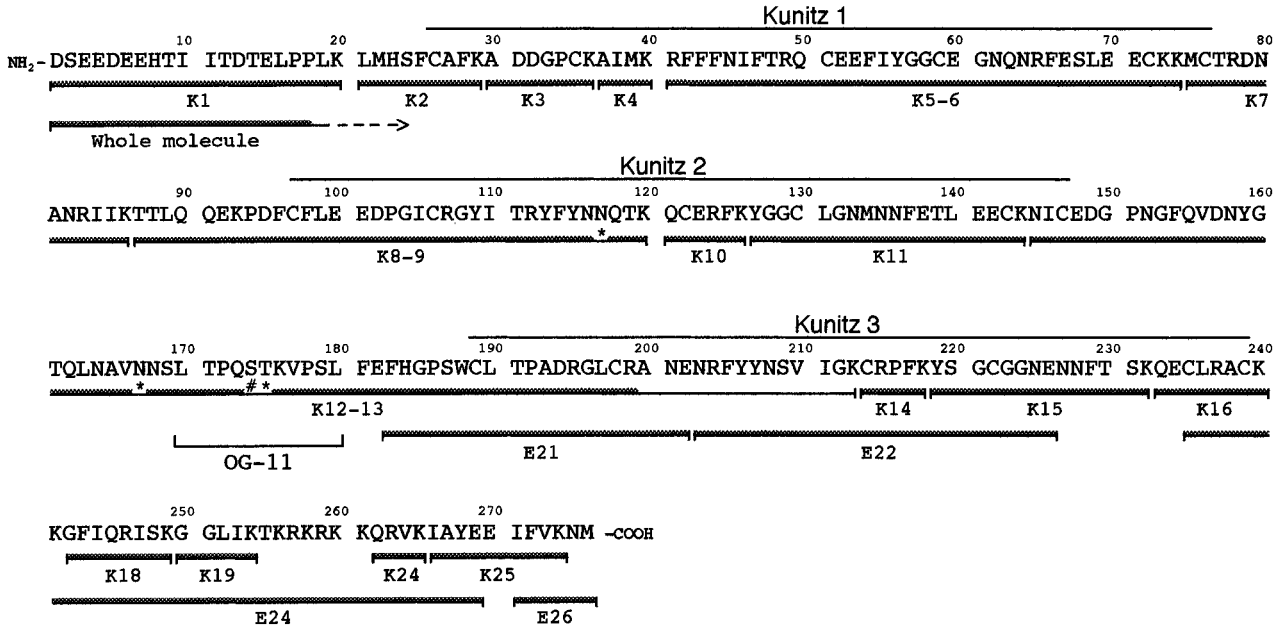

FIGURE 1: Amino acid sequence of recombinant human TFPI. K, lysylendopeptidase peptides; E, V8 protease peptides; thick gray bars, PTH-amino acids identified using a protein sequencer; *, no PTH-amino acid was identified; #, the yield of PTH-amino acid was extremely low.

Two-Dimensional Sugar Mapping Analysis of N-Linked Carbohydrate Chains. The structures of *N*-linked carbohydrate chains were analyzed by means of two-dimensional sugar mapping (Tomiya et al., 1988) using RP-HPLC (PALPAK Type-R, Takara Shuzo Co., Ltd., or Nakano ODS-A, Nakano Vinegar Co., Ltd.) and size-fractionation HPLC (TSK-GEL Amide-80, Tosoh Co., Tokyo). The PA-carbohydrate chains derived from peaks H and I, and their glycosidase digests were analyzed by PALPAK Type-R and those from other peaks were analyzed by NAKANO ODS-A. The samples were eluted from PALPAK Type-R using a linear gradient from 5% to 55% solvent B for 100 min at 40 °C at a flow rate of 1.0 mL/min or eluted from Nakano ODS-A and TSK-GEL Amide-80 as described by Tomiya et al. (1988). Carbohydrate chains were identified using a fluorescence detector with excitation at 320 nm and emission at 400 nm. Elution positions of PA-carbohydrate chains were normalized by the elution positions of PA-glucose oligomers (Takara Shuzo, Co., Ltd.) and expressed as glucose units. The peak area was used to calculate the percentage of each carbohydrate chain, since the relative fluorescence is the same on a molar basis for each component (Hase et al., 1984).

Glycosidase Digestion of Asialo PA-Carbohydrate Chains. Asialo PA-carbohydrate chains were digested with β-galactosidase, β-*N*-acetylhexosaminidase, and α-fucosidase as described (Tomiya et al., 1987; Tsuda et al., 1988). Digestion with endo-β-galactosidase (10 milliunits) proceeded in 15 μL of 0.1 M acetate buffer (pH 5.8). Digestion with β-galactosidase (2.5 milliunits) and β-*N*-acetylhexosaminidase (10 milliunits) simultaneously proceeded in 15 μL of 0.1 M citrate-phosphate buffer (pH 4.5) and that with β-*N*-acetylhexosaminidase (10 milliunits) and endo-β-galactosidase (5 milliunits) in a mixture of 7.5 μL of 0.1 M citrate-phosphate (pH 5.0) and 7.5 μL of 0.1 M acetate buffers (pH 5.8). All digestions were performed at 37 °C for 15 h, and the reactions were stopped by boiling the solutions at 100 °C for 5 min. The digested carbohydrate chains were analyzed by RP-HPLC and size fractionation HPLC as described above.

Numbering of Carbohydrate Chains. The code numbering of carbohydrate chains is based on that reported by Tomiya et al. (1988).

Homology Search. The amino acid sequence, Pro^{151}—Phe^{181}, of human TFPI encoded by exon 7, was compared with 121 043 sequences stored in the PIR and the SWISS PROT Protein Sequence Databases using the algorithm of the computer program BLASTP (Altschul et al., 1990).

RESULTS

Amino Acid Sequence Analysis. Reduced and *S*-pyridylethylated r-hTFPI was digested with lysylendopeptidase or V8 protease. The lysylendopeptidase digest was separated by RP-HPLC. The V8 protease digest was first separated into four fractions by gel-filtration through Tosoh G3000SW. Each fraction was examined by RP-HPLC. The major portion (about 90%) of the amino acid sequence of r-hTFPI was determined using 17 peptides isolated from the lysylendopeptidase digests. The remainder was determined using four peptides from the V8 protease digests. The results of the sequence analysis are summarized in Figure 1. The amino acid sequence was identical to that predicted from the cDNA sequence. As reported previously, the actual and predicted amino acid compositions of r-hTFPI were also identical (Enjyoji, et al., 1995). These results indicated that the r-hTFPI is a full-length molecule with 276 amino acid residues.

There is a phosphorylated Ser residue at position 2 (Ser^2) in the TFPI produced by HepG2 cells and in the recombinant TFPI expressed in murine fibroblast C127 cells (Girard et al., 1990). Here, the amino acid sequence analysis of peptide K1 and the entire molecule showed that the yield of PTH-Ser at second cycle of Edman degradation was not decreased. The mass spectrum of peptide K1 showed a molecular mass of 2310.9 amu (data not shown), which is almost the same as calculated mass of peptide K1 without phosphorylation (2311.4 amu). These data suggested that the r-hTFPI expressed in CHO cells was not phosphorylated at Ser^2.

Table 1: Amino Acid and Carbohydrate Compositions and Amino Acid Sequence of Peptide OG-11

amino acid composition[a]	
Glx 1.4 (1), Ser 2.4 (2), Thr 2.1 (2), Pro 2.0 (2), Val 0.9 (1), Leu 1.8 (2), Lys 0.9 (1)	
carbohydrate composition[a]	
GalNAc 1.9 (2), Gal 2.2 (2)	
amino acid sequence[b]	
Leu-Thr-Pro-Gln-XXX-XXX-Lys-Val-Pro-Ser-Leu	
55 15 37 25	21 30 22 4 8

[a] Numbers in parentheses represent rounded values. [b] XXX: not identified. Yield of PTH amino acids is expressed in picomoles.

Structural Analysis of O-Linked Carbohydrate Chains. The neutral and amino sugar composition analyses of whole r-hTFPI molecule showed that the sugar ratio of GalNAc: GlcNAc:Man:Fuc:Gal was 1.9:7.3:3.0:1.2:5.9. The presence of GalNAc indicated that there are *O*-linked carbohydrate chains in r-hTFPI. A lysylendopeptidase peptide, K12−13, corresponding to Asn^{145}−Lys^{213}, has a potential lysylendopeptidase cleavage site at Lys^{176}. However, it was not cleaved. Sequence analysis of the peptide K12−13 showed that yield of PTH-Ser at Ser^{174} was low and PTH-Thr at Thr^{175} was undetectable. These results suggest that Ser^{174} was partially and Thr^{175} fully *O*-glycosylated.

To obtain a shorter peptide carrying Ser^{174} and Thr^{175}, peptide K12−13 was digested with thermolysin and the digest was separated by RP-HPLC. Aliquots of each peak were acid hydrolyzed to detect GalNAc and it was found in peptide OG-11 (Figure 1). The amino acid composition and sequence of peptide OG-11 (Table 1) showed that it was an undecapeptide, corresponding to Leu^{170}−Leu^{180}, in which both Ser^{174} and Thr^{175} were glycosylated. About 2 mol of GalNAc and Gal were detected per mol of peptide OG-11 (Table 1). These data suggested that *O*-linked carbohydrate chains with a type-1 core structure, Gal-GalNAc-Ser/Thr, were attached to Ser^{174} and Thr^{175}, respectively, although the sialic acid content was not analyzed.

We confirmed the structure of *O*-linked carbohydrate chains by means of ion spray mass spectrometry of peptide OG-11. Several signals with *m*/*z* of 1388.4, 1242.8, 1161.8, 1097.2, and 1016.2, were identified (Figure 2). These ions were doubly charged according to an isotopic distribution of them. The calculated molecular mass of these ions were 2774.8, 2483.6, 2321.6, 2192.4, and 2030.4 Da, respectively. The multiple ions resulted either from the heterogeneity of the glycopeptide OG-11 or from fragmentation of the oligosaccharide chains in the orifice of the mass spectrometer. The calculated molecular weight of the polypeptide chain of OG-11 was 1170.4 Da. The observed ion with *m*/*z* 1388.4 (molecular mass: 2774.8) corresponded to the mass of OG-11 with 2 mol of HexNAc, 2 mol of Hex, and 3 mol of NeuAc. Other ions were attributable to the losses of NeuAc and/or Hex as shown in Figure 2.

The doubly charged parent ion of *m*/*z* 1388.4 was analyzed by tandem mass spectrometry (Figure 3). Many daughter ions were detected, and the charge state of the daughter ions was confirmed from their isotopic distribution, Fragments tagged with "#" were doubly charged. The presence of 2 mol of HexNAc, 2 mol of Hex, and 3 mol of NeuAc was confirmed from the pattern between doubly-charged ions at

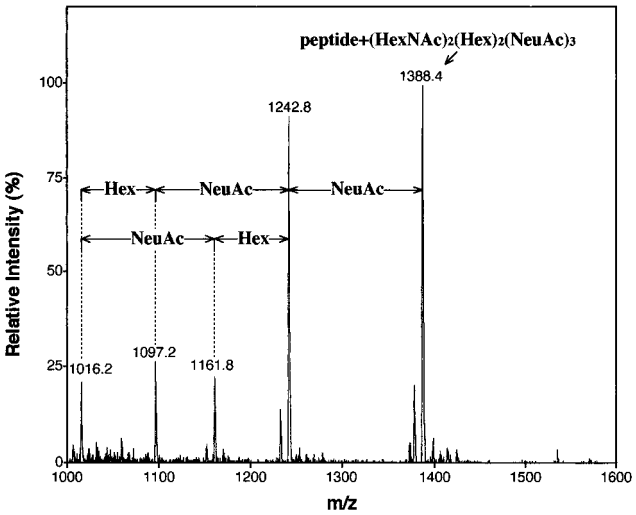

FIGURE 2: Ion spray mass spectrum of glycopeptide OG-11. The positive-ion spectrum was obtained between 1000 and 1600 Da. Step size, 0.1 amu; dwell time, 1 ms per step; ionspray voltage, 5000 V, and orifice potential, 90 V.

m/*z* 586.0 (peptide portion) and at *m*/*z* 1388.2 (parent ion) and from the pattern of singly-charged ions over *m*/*z* 1170.6. Fragment ions at *m*/*z* 687.5 and 1373.8 were assigned to be peptides with only HexNAc. However, no signal corresponded to the glycopeptide with only Hex, calculated *m*/*z* of 1333 (singly charged), or 667 (doubly charged). Therefore, the *O*-linked carbohydrate chains were confirmed to be the type 1 core structure attached by HexNAc. The singly-charged small ions, from *m*/*z* 203.9 to 657.2, were attributed to the oxonium ions of a monosaccharide or a carbohydrate chain released from the peptide portion, which supports the above carbohydrate structures. The glycosyl linkage of NeuAc could not be completely determined. However, NeuAc-HexNAc and NeuAc-Hex linkages were suggested by carbohydrate oxonium ions at *m*/*z* 495.1 and 454.3, which corresponded to the mass of one HexNAc plus one NeuAc and to one Hex plus one NeuAc, respectively.

The sugar composition, amino acid sequence, and mass spectrometric analyses demonstrated that the undecapeptide OG-11 is a glycopeptide with the two *O*-linked carbohydrate chains that consist of the type-1 core structure at Ser^{174} and Thr^{175}.

Structural Analysis of N-Linked Carbohydrate Chains. Human TFPI has three potential *N*-glycosylation sites. Amino acid sequence analyses of peptides K8−9 and K12−13 from the lysylendopeptidase digest revealed that Asn^{117} and Asn^{167} were almost fully glycosylated because PTH-Asn was not detected at those positions (Figure 1). In contrast, PTH-Asn was clearly detected on Asn^{228} of K15. These results suggested that one of the three potential *N*-glycosylation sites, Asn^{228}, was not glycosylated.

To analyze the structure of the *N*-linked carbohydrate chains, PA-derivatized *N*-linked carbohydrate chains were obtained from r-hTFPI as described under Experimental Procedures and examined by means of anion-exchange HPLC, using a PALPAK Type-N column. The PA-carbohydrates from r-hTFPI were separated into more than fifty peaks. Under these conditions, PA-carbohydrate chains were separated mostly depending on their negative charge and partly on their structural differences. We compared the profile with those of authentic PA-carbohydrate chain

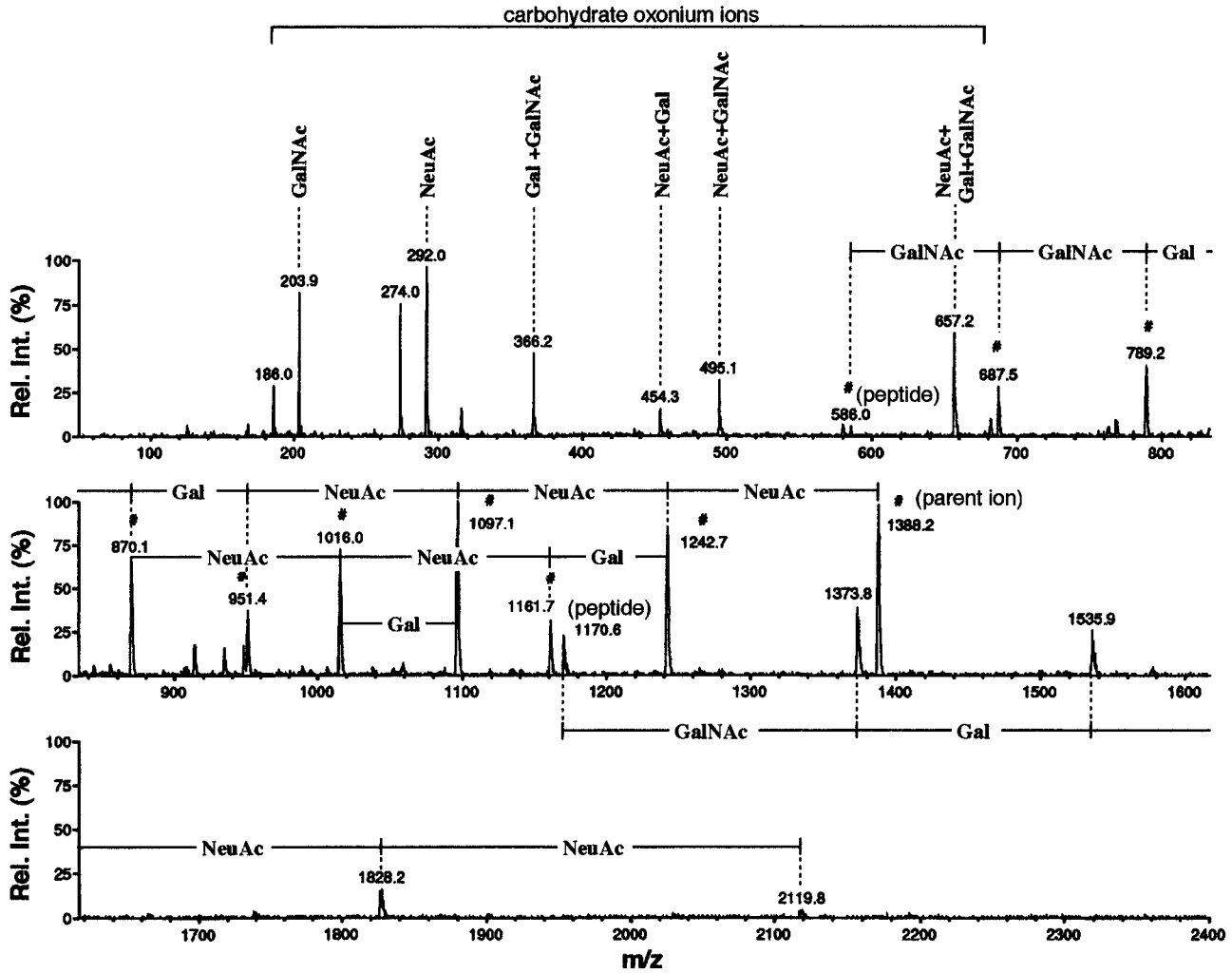

FIGURE 3: Daughter ion spectrum from the *m*/*z* 1388.4 in Figure 2. The spectrum was obtained between 50 and 2400 Da. Step size, 0.1 amu; dwell time, 1 ms per step; ionspray voltage, 5000 V, and orifice potential, 90 V. The collision energy was 20 V. The collision gas was argon, and the gas density was 2.8×10^{14} molecules/cm^2. Fragment ions marked by "#" were doubly protonated.

standards and PA-carbohydrate chains released from bovine fetuin (data not shown). The results indicated that the carbohydrate chains of r-hTFPI presumably consist mainly of monosialo (about 40% of total carbohydrate chains), some asialo and disialo (about 20%−30%, respectively), and few trisialo carbohydrate chains. After sialidase digestion, scattered peaks settled into the asialo fraction. This result suggests that all the negative charges of carbohydrate chains released from r-hTFPI expressed in CHO cells were carried by sialic acids, not by sulfation of the carbohydrate chains, although sulfated *N*-linked carbohydrate chains have been found on TFPI produced by rabbit arterial endothelial cells (Colburn & Buonassisi, 1988; Warn-Cramer et al., 1991) and recombinant TFPI expressed in human kidney 293 cells (Smith et al., 1992).

A completely asialated PA-carbohydrate chain mixture was separated by RP-HPLC (Figure 4), and the eight major peaks, named C, D, E, H, I, J, M, and O, were analyzed by the two-dimensional sugar mapping combined with sequential glycosidase digestion as described under Experimental Procedures. The carbohydrate structures of these PA-carbohydrate chains were elucidated by glycosidase digestion as indicated in Figure 5. The glucose units of each digest on size-fractionation and RP-HPLC were compared with those of standard PA-carbohydrate chains or with those reported by Tomiya et al. (1988). PA-carbohydrate chains

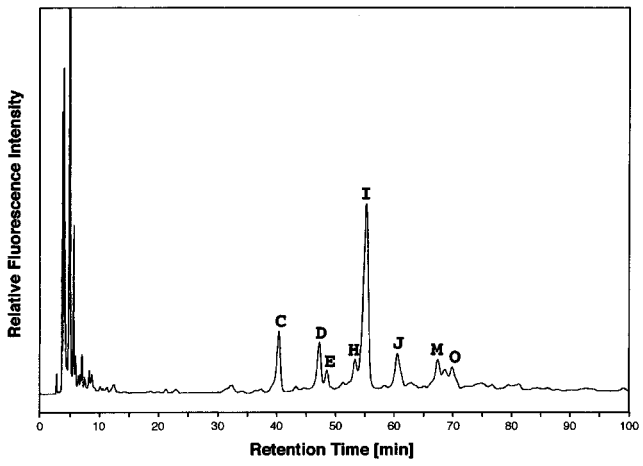

FIGURE 4: The elution profile of asialated PA-carbohydrate chains obtained from r-hTFPI on RP-HPLC using Takara PALPAK Type-R. PA-derivatives of *N*-linked carbohydrate chains were prepared and digested with sialidase as described under Experimental Procedures. The chromatographic conditions are also as described under Experimental Procedures.

and their glycosidase digests from peaks H, I, and O were identified from the elution positions of standard PA-carbohydrate chains.

The elution position and the manner of glycosidase digestions suggested the carbohydrate structure from peak

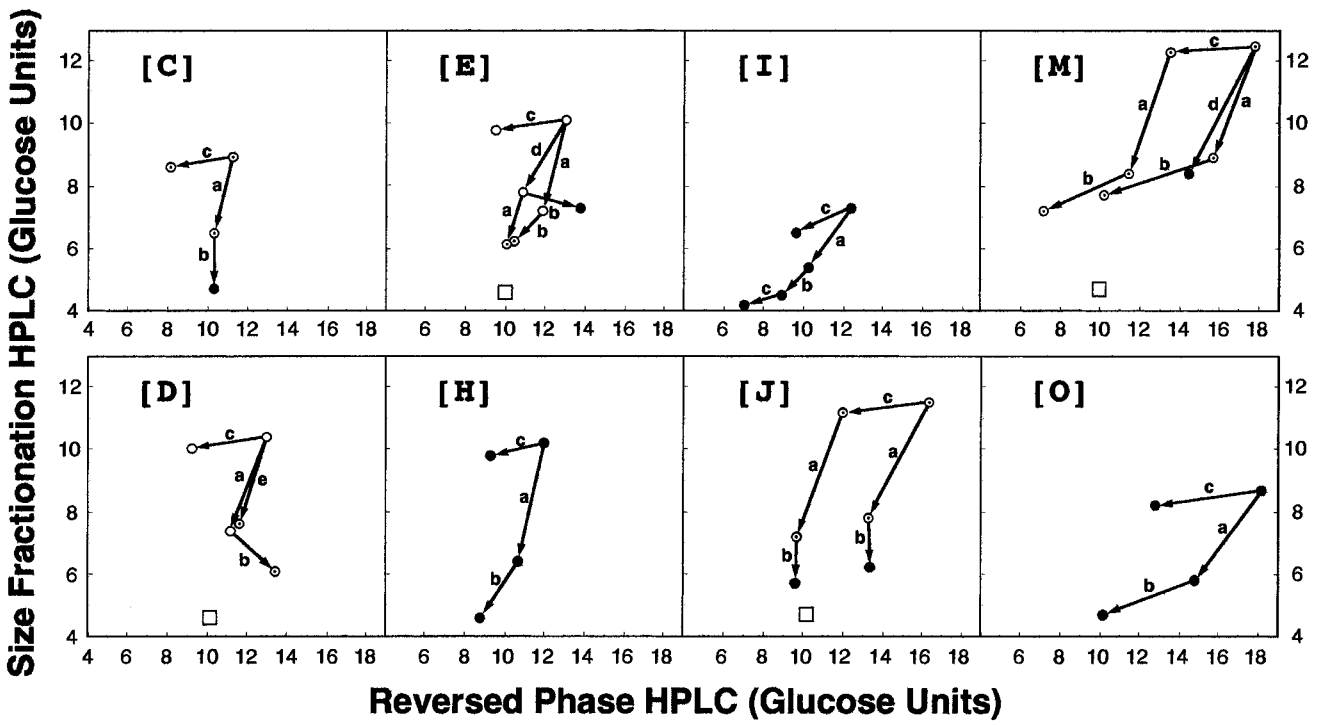

FIGURE 5: Two-dimensional sugar mapping of the PA-carbohydrate chains isolated in Figure 4. The scales are expressed in glucose units. Arrows indicate changes in elution positions after digestion with glycosidases: ($\xrightarrow{a}$), β-galactosidase; ($\xrightarrow{b}$), β-N-acetylhexosaminidase; ($\xrightarrow{c}$), α-fucosidase; ($\xrightarrow{d}$), endo-β-galactosidase, and ($\xrightarrow{e}$), endo-β-galactosidase with β-N-acetylhexosaminidase. Circles indicate the elution position of each PA-carbohydrate chain; ●, identified by co-elution with standard PA-carbohydrate chain; ⊙, identified by the elution position, referring to that reported by Tomiya et al. (1988); ○, the elution position of PA-carbohydrate chain not reported; (□), elution position after simultaneous digestion with β-galactosidase and β-*N*-acetylhexosaminidase.

C to be the known triantennary complex-type carbohydrate chain of code number 310.18, having three branches, Galβ1-4GlcNAcβ1-6, Galβ1-4GlcNAcβ1-2 linked to Manα(1-6), and Galβ1-4GlcNAcβ1-2 linked to Manα(1-3), each of which attached to the fucosyl trimannosyl core. However, three other structures could be possible for the structure of peak C, depending on branching of the core. One of the candidates was a fucosyl triantennary carbohydrate chain of code number 310.8. But the possibility was excluded by its different elution position on reversed phase HPLC (17.7 glucose units). The elution position of the second candidate, code number 310.19 (Tomiya et al., 1993), having Galβ1-4GlcNAcβ1-6 and Galβ1-4GlcNAcβ1-2 branches linked to Manα(1-6) and Galβ1-4GlcNAcβ1-4 branch to Manα(1-3), is very close to that of code number 310.18 (310.18 = 11.2/9.0 vs 310.19 = 11.4/9.2 glucose units on ODS/Amide). Furthermore, the elution position of the third candidate, having Galβ1-4GlcNAcβ1-6 branch linked to Manα(1-6) and Galβ1-4GlcNAcβ1-4 and Galβ1-4GlcNAcβ1-2 branches to Manα1-3, had not been reported. In order to confirm the structural assignment, the intact PA-derivative from peak C was completely digested with β-galactosidase, and then the digest was subjected to partial digestion with β-*N*-acetylhexosaminidase. The digest was separated by size-fractionation HPLC (Amide-80), and the mono-GlcNAc fraction (5.0−5.3 glucose units) was collected. This fraction was analyzed by reversed phase HPLC (ODS-A). As a result, three types of mono-GlcNAc components were obtained. Their elution positions were 12.7/5.1, 10.3/5.3, and 10.2/5.1 glucose units on the ODS/Amide column, which corresponded to those of carbohydrate numbers, 110.1, 110.6, and 110.2, respectively. These published structures are one GlcNAc linked by β1-2 and by β1-6 to the Man(α1-6) arm of fucosyl trimannosyl core and by β1-2 to Man(α1-3), respectively. If peak C was number 310.19 or the unpublished structure described above, the mono-GlcNAc compound (number 110.7, 11.0/5.0 glucose unit), one GlcNAc linked to the Man(α1-3) arm by β1-4 linkage, should have been observed, instead of number 110.2 or 110.1. On the basis of these results, the carbohydrate structure from peak C was assigned as code number 310.18 and shown in Table 2.

In contrast with peaks C, H, I, and O, PA-carbohydrates from peaks D, E, J, and M were not converted into the core after the subsequent digestion with β-galactosidase and with β-*N*-acetylhexosaminidase. However, they were converted into core structures by simultaneous digestion by these two glycosidases, which released both Gal and GalNAc residues despite of the repeated structure of Galβ1-4GlcNAc residues (LacNAc). On the other hand, they were susceptible to *E. freundii* endo-β-galactosidase, which recognizes specifically LacNAc repeat structure and converts R-GlcNAcβ1-3Galβ1-4GlcNAc-R′ into R-GlcNAcβ1-3Gal and GlcNAc-R′ (Spooncer et al., 1984; Fukuda et al., 1984). These results suggested that carbohydrate chains from peaks D, E, J, and M were complex-type with LacNAc tandem repeat(s).

The elution positions of the PA-carbohydrate chain from peak J and its glycosidase digests were the same as those of the tetraantennary carbohydrate chain (number 410.42), which has one LacNAc repeat on the GlcNAc(β1-2) branch attached to the Man(α1-6) arm of the fucosyl trimannosyl core. The elution positions of the PA-carbohydrate chain from peak M and its digests were the same as those of the carbohydrate chain (number 410.52), which has LacNAc repeats on both branches of Man(α1-6). The carbohydrate chains from peaks D and E were supposed to be fucosyl

Table 2: Elucidated Structures of *N*-Linked Carbohydrate Chains in r-hTFPI[a]

PA-carbohydrate chain (Abbreviation)	Structure	Amount (%)
[I]	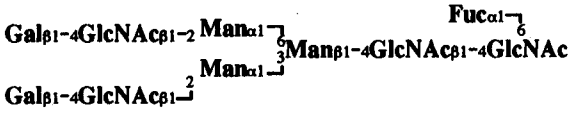	34.6
[C]	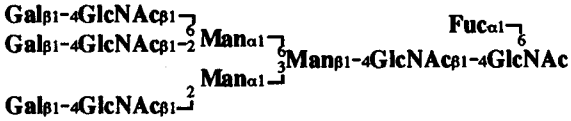	9.3
[D]	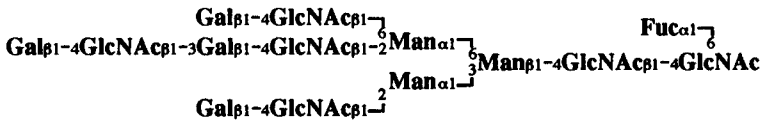	7.8
[E]	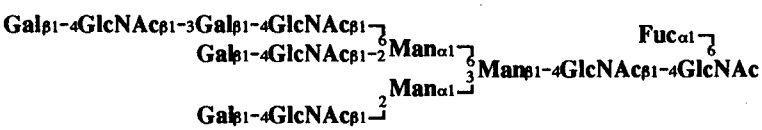	2.8
[O]	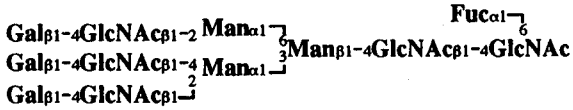	4.8
[H]		5.6
[J]	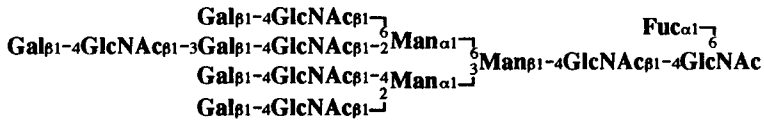	7.2
[M]	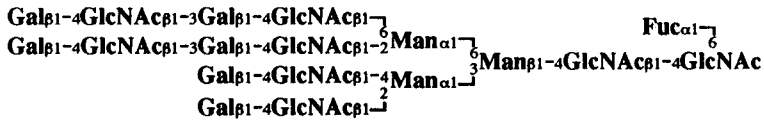	5.8
	Total	77.9

[a] The structures of eight major peaks of PA-carbohydrate chains from Figure 4 were determined as shown in Figure 5. The relative amounts of the carbohydrate chains were calculated from the peak areas in Figure 4.

triantennary complex-type with one or more tandem LacNAc repeats, but their mapping data did not correspond to those previously reported. We therefore examined these structures by using glycosidase digstions in combination with endo-β-galactosidase. A branch without one or more LacNAc repeat is lost after subsequent digestion with β-galactosidase and with β-*N*-acetylhexosaminidase, whereas a branch with LacNAc repeat is removed by the subsequent digestion with β-*N*-acetylhexosaminidase and with endo-β-galactosidase or by the simultaneous digestion of these two glycosidases. The elution position of PA-carbohydrate chain from peak D was the same as that of number 110.3, one Galβ1-4GlcNAc linked to the Man(α1-6) arm of fucosyl trimannosyl core by β1-2 linkage, after the subsequent digestion with β-galactosidase and with β-*N*-acetylhexosaminidase, and as that of number 210.12, two Galβ1-4GlcNAc linked to Man(α1-6) by a β1-6 and to Man(α1-3) by β1-2, after the simultaneous digestion with these two glycosidases. These results indicate that one LacNAc repeat existed on the β1-2 branch of the Man(α1-6), Galβ1-4GlcNAc residues linked to Man(α1-6) by β1-6 linkage, and linked to Man(α1-3) by β1-2. In the same way, the carbohydrate structure from peak E was determined. The carbohydrate derivative was identified to be code number 110.8 after the subsequent digestion with

β-galactosidase and with β-*N*-acetylhexosaminidase, and to be code number 210.4 after the subsequent digestion with endo-β-galactosidase and with β-*N*-acetylhexosaminidase. These results indicate that the carbohydrate chain from peak E was fucosyl triantenna having LacNAc repeated branch linked to Man(α1-6) by β1-6 linkage, as shown in Table 2.

All of the carbohydrate chains were of the complex-type with one α1-6 linked fucose residue attached to reducing-end GlcNAc. The main component (peak I) was a biantennary carbohydrate chain. Triantennary (peaks C, D, E, and O) and tetraantennary (peaks H, J, and M) carbohydrate chains were also identified. Some of the triantennary and tetraantennary carbohydrate chains (peaks D, E, J, and M) had one or two LacNAc repeats (30% of *N*-linked carbohydrates structurally determined).

DISCUSSION

This study showed that the r-hTFPI from CHO cells was a full-length glycoprotein with two *N*-glycosylation sites (Asn^{117} and Asn^{167}) among three potential glycosylation sites and with two *O*-glycosylation sites (Ser^{174} and Thr^{175}). Although no clear rule has been established for *O*-glycosylation sites, a proline residue at +3 reportedly makes *O*-glycosylation favorable (Dwek, 1995). In fact, proline was located at +3 of Thr^{175}. No evidence of other post-translational modification was found, such as phosphorylation at Ser^{2} as reported by Girard et al. (1990). The Asn^{117} in Kunitz domain 2 was *N*-glycosylated, whereas Asn^{228}, one of three potential *N*-glycosylation sites, in Kunitz domain 3 was not. Since the carbohydrate chain at Asn^{117} locates near the reactive site of Kunitz domain 2, it may influence the function of the domain.

All of the *N*-linked carbohydrate chains in r-hTFPI were complex-type carbohydrate chains with one fucose residue attached to the reducing-end GlcNAc. They consisted of biantennary (44.4% of the chains determined), triantennary (31.7%), and tetraantennary (23.9%) carbohydrate structures. Since these branched structures are formed depending mainly on the amino acid sequence and conformation of proteins (Takeuchi & Kobata, 1991), the same distribution of the branched structures is supposed to be found in plasma-derived TFPI. Their non-reducing ends featured a LacNAc repeat (about 30% of the carbohydrate chains determined). This is often found in recombinant proteins from CHO cells, e.g., erythropoietin (Takeuchi et al., 1988), interferon-β1 (Kagawa et al., 1988), gp120 from human immunodeficiency-virus (Mizuochi et al., 1988), and interleukin-6 (Orita et al., 1994). Although the role of the LacNAc repeat has not been established, Fukuda et al. (1989) have suggested that it is related to the metabolism of the glycoproteins in liver. Since this repeat is supposed to be characteristic of recombinant proteins from CHO cells, our results do not necessarily mean that plasma-derived TFPI has this structure. Although we did not examine the sialyl bonds of *N*-linked carbohydrate chains in r-hTFPI, NeuAcs are supposed to be attached to Gal by α2-3 linkages, since almost all of *N*-linked carbohydrates in the recombinant proteins from CHO cells have the α2-3 linkages.

Since *N*-linked carbohydrate chains from r-hTFPI lost their negative charge after sialidase digestion, we found no evidence to support the presence of sulfated carbohydrate chains as found on rTFPI from human kidney 293 cells (Smith et al., 1992). *N*-Linked sulfated carbohydrate chains are generated by a combination of a specific GalNAc-transferase and 4-sulfotransferase. Smith et al. have speculated that a sulfated carbohydrate chain is linked to Asn^{228}, since the recognition sequence, Pro-Phe-Lys, for GalNAc-transferase has been found at the *N*-terminal of Asn^{228}. However, evidence has not been directly presented for the presence of *N*-glycosylation at Asn^{228} of rTFPI from 293 cells. In addition, they found that $[^{35}S]SO_4$ was incorporated into TFPI expressed in human kidney 293 cells but not in CHO or HepG2 cells. Our finding that Asn^{228} in r-hTFPI from CHO cells was not glycosylated is consistent with their results.

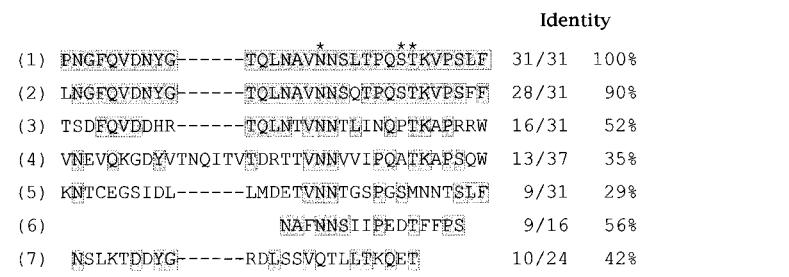

FIGURE 6: Comparison of amino acid sequence and glycosylation sites of the region encoded by human TFPI exon 7 with the corresponding regions of TFPI from monkey, rabbit, rat, and dog and with homologous sequence in other proteins. The identical amino acid residues with those of human TFPI are shaded. The numbers of the identical amino acid residues per total amino acid residues and the percentages are also shown. (1) Human TFPI 151−181 (Wun et al., 1988); (2) monkey TFPI 151−181 (Kamei et al., 1994); (3) rabbit TFPI 152−182 (Wesselschmidt et al., 1990); (4) rat TFPI 149−185 (Enjyoji et al., 1992); (5) canine TFPI 144−174 (Girard et al., 1994); (6) human T-cell receptor α chain C region (142 residues), 76−91 (Yanagi et al., 1985); (7) human non-erythroid spectrin (fodrin) α chain (2472 residues) 1997−2020 (Moon & McMahon, 1990). "*" marks glycosylation sites found in r-hTFPI.

The structure of *O*-linked carbohydrate chains in r-hTFPI was determined to be a type-1 core structure with sialic acids. This type of *O*-linked carbohydrate chain is found in the activation peptide portion of human factor IX (Agarwala et al., 1994) and many recombinant proteins (Inoue et al., 1993; Tsuda et al., 1990; Sasaki et al., 1987; Oheda et al., 1988; Kodama et al., 1993). The failure of lysylendopeptidase to cleave the Lys^{176}−Val^{177} bond indicated that the two *O*-glycosyl carbohydrate chains at Ser^{174} and Thr^{175} interfered with the interaction of the protease with r-hTFPI. In addition to the two *O*-glycosylated sites, the presence of a carbohydrate chain at Asn^{167} will also influence the susceptibility of this region between Kunitz domains 2 and 3 toward various proteases. We compared the amino acid sequence of this carbohydrate-rich region encoded by exon 7 (van der Logt et al., 1991; Girard et al., 1991; Enjyoji et al., 1993) with the corresponding regions of TFPI from other species (Kamei et al., 1994; Wesselschmidt et al., 1990; Enjyoji et al., 1992; Girard et al., 1994). The homology with human TFPI was striking in that from monkey, rabbit, rat and dog, with an identity of 29 to 90% (Figure 6). The potential *N*-glycosylation site, Asn^{167}, was found in TFPI from all species reported except in rat TFPI. The potential *O*-glycosylation site, Thr^{175}, was also found in TFPI from all these species except the dog. The potential *O*-glycosylation site, Ser^{174}, was found in TFPI from monkey and dog. These results suggest that TFPI from all of these species has a carbohydrate-rich region between Kunitz domains 2 and 3, like human

TFPI. Although the cluster of carbohydrate chains in this region presumably influences the conformation of TFPI and its susceptibility to proteases, the significance of this carbohydrate-rich region remains to be established. Leukocyte elastase preferentially cleaves a peptide bond between Kunitz domains 1 and 2 of r-hTFPI (Higuchi et al., 1992), while proteases cleaving other regions in TFPI have not been identified. On the other hand, Broze et al. (1994) suggested the presence of carboxy-terminally truncated forms of TFPI in normal plasma, which deleted both the carboxy-terminal basic domain and Kunitz domain 3. It is of interest to know which proteases generated these truncated forms of TFPI, if the presence of three bulky and acidic carbohydrate chains in the region between Kunitz domains 2 and 3 of plasma-derived TFPI is assumed. As shown in Figure 6, the amino acid sequence encoded by human exon 7 has a striking identity with the C-region of the human T-cell receptor α chain (Yanagi et al., 1985) and the human non-erythroid spectrin (fodrin) α chain (Moon & McMahon, 1990), in which Thr residues corresponding to Thr^{175} were preserved.

Studies on the structure of the carbohydrate chains of several recombinant proteins, have established that the carbohydrate structures of recombinant glycoproteins are also dependent on the cell-types used for the expression of the recombinant proteins. Among various mammalian cells, CHO cells synthesize recombinant proteins with carbohydrates similar to human counterparts (Utsumi et al., 1989; Kagawa et al., 1988; Hara et al., 1993). Therefore, the present findings of the glycosylation sites and the branched structures of carbohydrates of r-hTFPI can be generally applied to plasma-derived TFPI, although those of plasma TFPI and endothelial cell-associated TFPI should be determined. Particularly, sulfation of *N*-linked carbohydrates in plasma-derived TFPI should be examined more in detail, since that of TFPI produced by human umbilical endothelial cells has been described (Broze et al., 1990). In any event, the present information may facilitate understanding of the various functions of TFPI, such as the inhibition of factor Xa and tissue factor−factor VIIa, interactions with lipoproteins, proteoglycans, and heparin, as well as the susceptibility toward proteases in plasma and leukocytes.

ACKNOWLEDGMENT

We are grateful to Drs. Nahoki Kuraya, Tomohiro Mega, and Sumihiro Hase, Department of Chemistry, Osaka University College of Science, for the guidance in pyridylamination of the sugar chains.

REFERENCES

Agarwala, K. L., Kawabata, S., Takao, T., Murata, H., Shimonishi, Y., Nishimura, H., & Iwanaga, S. (1994) *Biochemistry 33*, 5167−5171.

Altschul, S. F., Gish, S. F., Miller, W., Myers, E. W., & Lipman, D. J. (1990) *J. Mol. Biol. 215*, 403−410.

Broze, G. J., Jr. (1995) *Annu. Rev. Med. 46*, 103−112.

Broze, G. J., Jr., Girard, T. J., & Novotny, W. F. (1990) *Biochemistry 29*, 7539−7546.

Broze, G. J., Jr., Lange, G. W., Duffin, K. L., & MacPhail, L. (1994) *Blood Coagulation Fibrinolysis 5*, 551−559.

Colburn, P., & Buonassisi, V. (1988) *In Vitro Cell. Dev. Biol. 24*, 1133−1136.

Diaz-Collier, J. A., Palmier, M. O., Kretzmer, K. K., Bishop, B. F., Combs, R. G., Obukowicz, M. G., Frazier, R. B., Bild, G. S., Joy, W. D., Hill, S. R., Duffin, K. L., Gustafson, M. E., Junger, K. D., Grabner, R. W., Galluppi, G. R., & Wun, T.-C. (1994) *Thromb. Haemostasis 71*, 339−346.

Dwek, R. A. (1995) *Biochem. Soc. Trans. 23*, 19−43.

Enjyoji, K., Emi, M., Mukai, T., & Kato, H. (1992) *J. Biochem. 111*, 681−687.

Enjyoji, K., Emi, M., Mukai, T., Leppert, M. L., & Lalouel, J. M. (1993) *Genomics 17*, 423−428.

Enjyoji, K., Miyata, T., Kamikubo, Y., & Kato, H. (1995) *Biochemistry 34*, 5725−5735.

Fukuda, M., Spooncer, E., Oates, J. E., & Dell, A. (1984) *J. Biol. Chem., 259*, 10925−10935.

Fukuda, M. N., Sasaki, H., Lopez, L., & Fukuda, M. (1989) *Blood 73*, 84−89.

Girard, T. J., McCourt, D., Novotny, W. F., MacPhail, L. A., Likert, K. M., & Broze, G. J., Jr. (1990) *Biochem J. 270*, 621−625.

Girard, T. J., Eddy, R., Wesselschmidt, R. L., MacPhail, L. A., Likert, K. M., Byers, M. G., Shows, T. B., & Broze, G. J., Jr. (1991) *J. Biol. Chem. 266*, 5036−5041.

Girard, T. J., Ailani, D., & Broze, G. J., Jr. (1994) *Biochem. J. 303*, 923−928.

Hara, H., Nakae, Y., Sogabe, T., Ihara, I., Ueno, S., Sakai, H., Inoue, H., Shimizu, S., Nakamura, T., & Shimizu, N. (1993) *J. Biochem. 114*, 76−82.

Hase, S., Ibuki, T., & Ikenaka, T. (1984) *J. Biochem. 95*, 197−203.

Heinrikson, R. L., & Meredith, S. C. (1984) *Anal. Biochem. 136*, 65−74.

Higuchi, D. A., Wun, T.-C., Likert, K. M., & Broze, G. J., Jr. (1992) *Blood 79*, 1712−1719.

Inoue, N., Takeuchi, M., Asano, K., Shimizu, R., Takasaki, S., & Kobata, A. (1993) *Arch. Biophys. Biochem. 301*, 375−378.

Kagawa, Y., Takasaki, S., Utsumi, J., Hosoi, K., Shimizu, H., Kochibe, N., & Kobata, A. (1988) *J. Biol. Chem. 263*, 17508−17515.

Kamei, S., Kamikubo, Y., Hamuro, T., Fujimoto, H., Ishihara, M., Yonemaru, H., Miyamoto, S., Funatsu, A., Enjyoji, K., Abumiya, T., Miyata, T., & Kato, H. (1994) *J. Biochem. 115*, 708−714.

Kodama, S., Tsujimoto, M., Tsuruoka, N., Sugo, T., Endo, T., & Kobata, A. (1993) *Eur. J. Biochem. 211*, 903−908.

Kondo, A., Suzuki, J., Kuraya, N., Hase, S., Kato, I., & Ikenaka, T. (1990) *Agric. Biol. Chem. 54*, 2169−2170.

Lindahl, A. K., Sandset, P. M., & Abildgaard, U. (1992) *Blood Coagulation Fibrinolysis 3*, 439−449.

Mizuochi, T., Spellman, M. W., Larkin, M., Solomon, J., Basa, L., & Feizi, T. (1988) *Biochem. J. 254*, 599−603.

Moon, R. T., & McMahon, A. P. (1990) *J. Biol. Chem. 265*, 4427−4433.

Novotny, W. F. (1994*) Semin. Thromb. Hemostasis 20*, 101−108.

Oheda, M., Hase, S., Ono, M., & Ikenaka, T. (1988) *J. Biochem. 103*, 544−546.

Orita, T., Oh-eda, M., Hasegawa, M., Kuboniwa, H., Esaki, K., & Ochi, N. (1994) *J. Biochem. 115*, 345−350.

Petersen, J. G. L., Meyn, G., Rasmussen, J. S., Petersen, J., Bjorn, S. E., Jonassen, I., Christiansen, L., & Nordfang, O. (1993) *J. Biol. Chem. 268*, 13344−13351.

Petersen, L. C., Valentin, S., & Hedner, U. (1995*) Thromb. Res. 79*, 1−47.

Sasaki, H., Bothner, B., Dell, A., & Fukuda, M. (1987) *J. Biol. Chem. 262*, 12059−12076.

Smith, P. L., Skelton, T. P., Fiete, D., Dharmesh, S. M., Beranek, M. C., MacPhail, L., Broze, G. J., Jr., & Baenziger J. U. (1992) *J. Biol. Chem. 267*, 19140−19146.

Spooncer, E., Fukuda, M., Clock, J. C., Oates, J. E., & Dell, A. (1984) *J. Biol. Chem. 259*, 4792−4801.

Suzuki, J., Kondo, A., Kato, I., Hase, S., & Ikenaka, T. (1991) *Agric. Biol. Chem. 55*, 283−284.

Takemoto, H., Hase, S., & Ikenaka, T. (1985) *Anal. Biochem. 145*, 245−250.

Takeuchi, M., & Kobata, A. (1991) *Glycobiology 1*, 337−346.

Takeuchi, M., Takasaki, S., Miyazaki, H., Kato, T., Hoshi, S., Kochibe, N., & Kobata, A. (1988) *J. Biol. Chem. 263*, 3657−3663.

Tomiya, N., Kurono, M., Ishihara, H., Tejima, S., Endo, S., Arata, Y., & Takahashi, N. (1987) *Anal. Biochem. 163*, 489−499.

Tomiya, N., Awaya, J., Kurono, M., Endo, S., Arata, Y., & Takahashi, N. (1988) *Anal. Biochem. 171*, 73−90.

Tomiya, N., Awaya, J., Kurono, M., Hanazawa, H., Shimada, I., Arata, Y., Yoshida, T., & Takahashi, N. (1993) *J. Biol. Chem. 268*, 113−126.

Tsuda, E., Goto, M., Murakami, A., Akai, K., Ueda, M., Kawanishi, G., Takahashi, N., Sasaki, R., Chiba, H., Ishihara, H., Mori, M., Tejima, S., Endo, S., & Arata, Y. (1988) *Biochemistry 27*, 5646−5654.

Tsuda, E., Kawanishi, G., Ueda, M., Masuda, S., & Sasaki, R. (1990) *Eur. J. Biochem. 188*, 405−411.

Utsumi, J., Mizuno, Y., Hosoi, K., Okano, K., Sawada, R., Kajitani, M., Sakai, I., Naruto, M., & Shimizu, H. (1989) *Eur. J. Biochem. 181*, 545−553.

Valentin, S., Nordfang, O., Bregnard, C., & Wildgoose, P. (1993) *Blood Coagulation Fibrinolysis 4*, 713−720.

van der Logt, C. P. E., Reitsma, P. H., & Bertina, R. M. (1991) *Biochemistry 30*, 1571−1577.

Warn-Cramer, B. J., Maki, S. L., & Rapaport, S. I. (1991) *Thromb. Res. 61*, 515−527.

Wesselschmidt, R. L., Girard, T. J., & Broze, G. J., Jr. (1990) *Nucleic Acids Res. 18*, 6440.

Wun, T.-C. (1995) in *Molecular Biology of Thrombosis and Hemostasis* (Roberts, H. R., & High, K. A., Eds.) pp 331−353, Marcel Dekker, New York.

Wun, T.-C., Kretzmer, K. K., Palmier, M. O., Day, K. C., Huang, M. D., Welsch, D. J., Lewis, C., Wolfe, R. A., Zobel, J. F., Lange, G. W., Frazier, R. B., Bild, G. S., Peel, M. A., Shell, R. E., Horn, N. A., Junger, K. D., Foy, B. A., Gustafson, M. E., Leimgruber, R. M., Novotny, W. F., Broze, G. J., Jr., Pyla, Y. E., Hippenmeyer, P. J., & Warren, T. G. (1992) *Thromb. Haemost. 68*, 54−59.

Yanagi, Y., Chan, A., Chin, B., Minden, M., & Mak, T. W. (1985) *Proc. Natl. Acad. Sci. U.S.A. 82*, 3430−3434.

BI9524880